LRET Investigations of Conformational Changes in the Ligand Binding Domain of a Functional AMPA Receptor †

ARTICLE *in* BIOCHEMISTRY · SEPTEMBER 2008

Impact Factor: 3.02 · DOI: 10.1021/bi800690b · Source: PubMed

Published in final edited form as:
Biochemistry. 2008 September 23; 47(38): 10027–10032. doi:10.1021/bi800690b.

LRET investigations of conformational changes in the ligand binding domain of a functional AMPA receptor

Jennifer Gonzalez, **Anu Rambhadran**, **Mei Du**, and **Vasanthi Jayaraman***
Center for Membrane Biology, Department of Biochemistry and Molecular Biology, University of Texas Health Science Center, Houston, Texas, 77030

Abstract

The structural investigations using the soluble ligand binding domain of the AMPA subtype of the glutamate receptor have provided invaluable insight into the mechanistic pathway by which agonist binding to this extracellular domain mediates the formation of cation-selective channels in this protein. These structures, however, are in the absence of the transmembrane segments, the primary functional component of the protein. Here, we have used a modified luminescence resonance energy transfer based method to obtain distance changes due to agonist binding in the ligand binding domain in the presence of the transmembrane segments. These distance changes show that the cleft closure conformational change observed in the isolated ligand binding domain upon binding agonist is conserved in the receptor with the channel segments, thus establishing that the isolated ligand binding domain is a good model of the domain in the receptor containing the transmembrane segments.

Keywords

LRET; glutamate receptor; Luminescence; Cleft closure; AMPA receptor

Most fast excitatory signaling in the mammalian brain is mediated by ionotropic AMPA-type glutamate receptors, with glutamate binding to an extracellular domain on the postsynaptic AMPA receptors leading to the opening of a cation-selective channel that results in depolarization of the receiving cell (1-5). Significant insight into the mechanism by which the agonist mediates receptor activation has been obtained by the large number of structural investigations on the isolated extracellular ligand binding domain (3,6-22). These structural investigations, in combination with the vast existing electrophysiological data on the native receptor (23-25), suggest that the cleft closure conformational change induced by agonist binding is one of the key coupling mechanisms between the ligand binding domain and the channel segments (3,16,20). While the structures of this isolated domain have provided invaluable insight into the allosteric mechanism, they are limited by the fact that the domain is isolated and in the absence of the functional ion channel segments. The limitation of the use of the isolated ligand binding domain is most evident in the case of the dimer interface. While functional and biochemical investigations clearly indicate that the dimer interface between two subunits breaks down in the glutamate-bound desensitized state (6), the crystal structures show an intact interface in the presence of glutamate (6). A structure similar to that of the desensitized state was only observed when a disulfide bond was introduced to force apart the dimer interface (15). While it is plausible that the cleft closure conformational change should be the same in both the isolated ligand binding domain and the domain in the presence of the functional

CORRESPONDING AUTHOR: Vasanthi Jayaraman, Center for Membrane Biology, Department of Biochemistry and Molecular Biology, University of Texas Health Science Center, 6431 Fannin St., Houston, Texas, 77030, Tel: 713-500-6236; Fax: 713-500-7444; E-mail: vasanthi.jayaraman@uth.tmc.edu..

transmembrane segments, there is still no direct evidence for this assumption. In order to validate the extensive investigations on the isolated ligand binding domain, it is essential to establish that the conformational changes observed in the isolated domain are also observed in this domain in the presence of the functional transmembrane segments.

We have previously used LRET measurements in a modified AMPA receptor to show that the ligand binding domain exhibited similar cleft closure conformational changes as the isolated ligand binding domain; however, this investigation was limited by the fact that the distance changes were measured with respect to GFP, which is nearly the same size as the ligand binding domain (26). Here, we have used LRET investigations between significantly smaller tags to show that the ligand-binding domain in a modified AMPA receptor (lacking the N terminal domain) which has the transmembrane segments, undergoes a similar cleft closure as that seen in the isolated ligand binding domain, thus confirming that the isolated ligand binding domain is a good model of the domain in the receptor. Since the AMPA receptors are not purified and are studied in a near physiological state (expressed in oocytes), we modified the LRET method by introducing a protease recognition or stop site between the acceptor site and the donor site of the protein of interest, thus allowing for the cleavage of the acceptor. Since the cleavage site is specific to the protein of interest, the action of the protease selectively removes the LRET signal from the protein of interest. Thus, the LRET signal measured after the cleavage provides a direct measure of the background non-specific LRET, which can be removed from the initial signal to obtain the LRET signal of interest (Figure 1). We first tested this modified LRET on the non-purified isolated ligand binding domain and compared the results to the purified protein to establish that the technique works on non-purified systems and then extended the methodology to investigate the changes in the AMPA receptor.

EXPERIMENTAL PROCEDURES

Modifications introduced in the GluR4 AMPA receptor expressed in Xenopus laevis oocytes

For studying the conformational changes in the ligand-binding domain of the AMPA receptor, we used a modified GluR4 subunit of the AMPA receptor lacking the N-terminal domain (residues 22-402) and with the two accessible cysteines (C426, C529) on the extracellular side mutated to serines, producing a modified AMPA receptor with no accessible cysteines. A cysteine was introduced at site 653 (corresponding to 652 in GluR2), and a hexahistidine tag was introduced at the N-terminus with a glutamine residue (P382Q) between the histag and the modified AMPA receptor sequence (histag-ΔN*-AMPA-S653C).

Mutant plasmid preparation

The plasmid for the soluble ligand binding domain of the AMPA receptor (GluR2-LBD) protein has been provided by Dr. Gouaux (Oregon Health and Science University, OR), and the plasmid for the GluR4-flip receptor with the first 402 residues deleted has been provided by Dr. Keinanen (University of Helsinki, Helsinki, Finland). The hexahistidine coding sequence was inserted into the N-terminal domain deleted GluR4 receptor after the viral signal peptide to replace the N-terminal flag epitope (27). For introducing the histag, the forward primer used was 104 bases in length with a *NheI* restriction site, signal peptide, and a hexahistidine tag followed by P382Q:
GGCTAGCTATAAATATGACTATTCTCTGCTGGCTTGCGCTGTTGTCAACACTTAC
CGCCGTGAACGCACACCATCATCATCATCACCAGACTCTGGGCAATGAC.

The backward primer contained an *EcoRI* restriction site,
CGGAATTCTTTTGTTGACCCAGAATCAAGT.

The PCR product was digested with *NheI* and *EcoRI* and subcloned into the corresponding sites of the ΔN*-AMPA receptor. Point mutations in the plasmids were introduced using the Stratagene QuikChange site-directed mutagenesis kit (Stratagene, CA). The integrity of the final constructs was verified by sequencing the coding region.

Expression of GluR2-LBD

Proteins were expressed, purified, and characterized as described by Armstrong *et al.* (8). In brief, the protein was expressed in *Escherichia coli* Origami-B(DE3) cells. Following clarification and concentration, the cell culture supernatant was used directly for the LRET measurements or purified by a Ni-NTA HiTrap affinity column and used for the LRET measurements. The supernatant or purified protein was labeled with maleimide derivatives of terbium chelate for donor only samples, and 5μM $(Ni\text{-}NTA)_2Cy3$ was added for donor:acceptor samples. 2.5 units of thrombin per mg of protein were added to the samples used for the LRET measurements, and the protein was maintained at 4°C. LRET measurements were performed 24 hours later. Parallel experiments with non-labeled protein before and after thrombin digestion were monitored by SDS gel electrophoresis to show selective cleavage of the GluR2-LBD protein by thrombin (supplementary figure 1).

Oocyte preparation

Oocytes were defolliculated by incubation of *Xenopus laevis* ovaries purchased from Nasco (WI) for 60–90 min with 1.5 mg/ml collagenase dissolved in Ca^{2+}-free solution containing (in mM): 83 NaCl, 2 KCl, 1 $MgCl_2$, 5 HEPES, pH 7.5. The preparation was thoroughly rinsed with storage solution containing (in mM): 88 NaCl, 2.5 $NaHCO_3$, 1.1 KCl, 0.4 $CaCl_2$, 0.3 $Ca(NO_3)_2$, 0.8 $MgCl_2$, 2.5 mM sodium pyruvate, 10 HEPES, pH 7.3, and 5 μg/ml gentamicin; and stored overnight. Stage V–VI oocytes were individually selected and injected with RNA of the modified mutant receptor.

Expression and tagging of the histag-ΔN*-AMPA-S653C receptor

The histag-ΔN*-AMPA-S653C receptor was expressed in oocytes by injecting the oocytes with RNA for this modified protein. After injection the oocytes were incubated for 2-3 days at 12°C and then pre-labeled to block the inherent cysteines with β-maleimidopropionic acid for 1 hour. This procedure has been used in LRET investigations of potassium channels and ensures that the background cysteines are blocked, thus increasing the specificity of fluorophore labeling (28,29). The blocked oocytes were placed at 18°C for 24 to 36 hours, allowing for the expression of the receptors. At the end of 24-36 hours, the oocytes were labeled with 2 μM maleimide terbium chelate for one hour. The excess fluorophore was then washed with storage solution. The oocyte membrane preparations obtained by lysis of these oocytes were used for western blotting, radioactive binding, and fluorescence measurements. For LRET experiments, approximately 300 healthy oocytes were lysed by gently douncing in 1.5 mL of lysis buffer, consisting of 20 mM Tris, pH 7.6, 200 mM NaCl, 1% Triton X-100, and EDTA-free Complete Protease Inhibitor Cocktail tablets (Roche Diagnostics, IN). Centrifugation was performed at 13,000 rpm for 10 minutes at 4°C to collect the supernatant. This procedure was repeated on the membrane samples for two more spins, and the resulting supernatant was used for the LRET experiments. To obtain the background LRET, the membrane preparations used for the fluorescence measurements were incubated with the dipeptidase (TAGzyme) obtained from Qiagen, Inc. CA. The TAGZyme system uses an exoproteolytic enzyme, DaPase (dipeptidyl aminopeptidase I), to cleave off N-terminal amino acids from proteins as dipeptides progressively until a defined stop point is reached. A glutamine inserted after the hexahistidine tag serves as the stop point in histag-ΔN*-AMPA-S653C. LRET was measured at 3 hours and 24 hours after the addition of the TAGzyme, and no significant changes were observed in the signal, suggesting that the peptidase reaction was complete in 3 hours at room temperature. To

demonstrate complete histag cleavage and an intact receptor expressed by *Xenopus* oocytes, western blotting was performed using membrane preparations treated with TAGZyme at different time points and probed with anti-penta histidine HRP conjugate (Qiagen, CA) or anti-GluR4 evolved towards the carboxy terminal peptide RQSSGLAVIASDLP (Millipore, MA) antibodies. The results indicate that after 3 hours at room temperature, TAGZyme histag digestion is complete (Supplementary Figure 2). Additionally, the expressed intact histag-ΔN*-AMPA-S653C construct was successfully probed by western blotting before and after TAGZyme digestion (Supplementary Figure 2).

Electrophysiological measurements

Two-electrode voltage-clamp experiments were performed using the NPI TEC amplifier (ALA Scientific, NY). Microelectrodes were filled with 3M KCl and had resistances of 1-3 MOhms. A narrow flow-through recording chamber with a volume of 75 μl was used to minimize the solution exchange time (ALA Scientific, NY). The extracellular solution contained (in mM): 100 NaCl, 1 KCl, 0.7 $BaCl_2$, 0.8 $MgCl_2$, and 5 HEPES, pH 7.5. Currents were recorded with Cell Works software (ALA Scientific, NY), and exported and analyzed using Origin 4.0 (OriginLab, MA).

Radioactive ligand binding measurements

The binding affinity of AMPA for the receptors was determined by saturation binding analysis using oocyte membranes. Constant amounts of membrane protein (12 μg) were incubated with increasing concentrations of [^{3}H]-AMPA. Bound and free radioligands were separated by rapid-filtration using Whatman nitrocellulose filters. Radioactivity was determined by counting with a liquid scintillation counter. Non-specific binding of [^{3}H]-AMPA was determined by including 10 mM glutamate in the binding assay. The K_d values for the ligands were determined by non-linear fitting of the binding data using equation 1:

$$y=\frac{x \times B_{max}}{x+K_d} \qquad \text{eq.1}$$

where y is the total binding of the radioactive ligand, B_{max} is the maximum amount of bound radioactive ligand, and x the concentration of free ligand.

Fluorescence spectroscopy

$(Ni\text{-}NTA)_2$-Cy3 was prepared as outlined in Kapanidis et al (30), and the terbium chelate was purchased from Invitrogen Corp. (CA). The fluorescence measurements were performed using a *TimeMaster*™ Model TM-3/2003 (Photon Technology International, NJ), a cuvette-based fluorescence lifetime spectrometer. The source was a nitrogen laser that is fiber-optically coupled to the sample compartment. Emitted light was collected and passed through a monochromator to a stroboscopic detector. Data was collected using Felix 32 software and analyzed using Origin software (OriginLab Corp. MA). The lifetimes typically were obtained by fitting an average of three to six sets of data. Prior to averages each individual data set was studied to ensure that it exhibits the same trends in the lifetimes. The donor only lifetimes were collected at 545 nm while the LRET lifetimes were obtained by studying the sensitized emission at 575 nm for Cy3.

Distance calculations based on lifetimes

The distance between the donor:acceptor fluorophores was determined by measuring the time constants of donor fluorescence decay in the absence acceptor and sensitized emission of the acceptor due to energy transfer from the donor using Förster's theory for energy transfer. R_0

was calculated as previously described (22). The errors reported in Table 1 include the error due to the orientation factor used in calculating the R_0 value. These errors were determined from the anisotropy measurements of the acceptor fluorophore using the calculations outlined by Haas et al. (31). The anisotropy of the acceptor molecule was measured using 10 μM GluR2-S1S2 with 50 nM $(Ni\text{-}NTA)_2Cy3$. These concentrations ensured that most of the $(Ni\text{-}NTA)_2Cy3$ was bound, and hence the anisotropy corresponded to the bound fluorophore. The anisotropy of the acceptor molecule under these conditions was determined to be 0.2, and that for the donor terbium chelate has been established to be 0 (32). It should be noted that the errors reported in Table 1 are the errors associated with the absolute distances; the relative errors between the various ligated states are expected to be less since the anisotropy of the donor and acceptor is the same between the various ligated states for a given donor:acceptor tagged protein.

RESULTS AND DISCUSSION

LRET to study non-purified systems

Prior to conducting the investigations on the AMPA receptor which exists in a non-purified environment, we investigated the isolated ligand binding domain of the AMPA receptors in a non-purified state, thus allowing us to compare the results from the non-purified protein to the previously reported studies on the purified system (22) and establish the feasibility of studying the receptor in a non-purified system. To study the non-purified isolated ligand binding domain, we tagged similar sites, the N-terminus and residue 652, as previously used for investigating the purified GluR2-LBD (6). The only modification was that the N-terminal histidine tag (acceptor binding site) was followed by a thrombin digestion sequence prior to the GluR2-LBD sequence. The protein was expressed in *E. coli*, and the supernatant of the cell lysate, without any further purification of the protein, was used for the LRET investigations. The supernatant was labeled with the maleimide derivative of terbium chelate and Ni-NTA derivative of Cy3 (30) (Figure 2). The lifetime of the sensitized emission of the acceptor due to energy transfer from the luminescent terbium chelate donor was measured before and after addition of thrombin, and the difference corresponding to the specific LRET between the cysteine and the histidine tag was obtained. This difference in lifetime could be well represented by a single exponential decay for both the apo (240 μs) and glutamate-bound (145 μs) forms of the protein (Figure 2; Table 1). Parallel investigations performed on the purified GluR2-LBD showed a smaller background LRET, and the lifetimes for the difference LRET were 210 μs and 130 μs for the apo and glutamate-bound states, respectively (Figure 2; Table 1). The good correlation between the LRET lifetimes obtained for the cell lysate and the pure protein clearly establish that the modification of introducing a protease site between the donor and acceptor allows for LRET investigations of unpurified systems.

Conformational changes in the receptor

Since these studies using the GluR2-LBD established the feasibility of the LRET measurements in measuring changes in a specific protein expressing a histidine tag with no requirement for purification, we extended these investigations to study the cleft closure conformational change in the ligand binding domain of a modified AMPA receptor expressed in oocytes. As outlined above, the previous structural investigations of this protein have been limited to the soluble extracellular domain (3,6,16,22,33). While these structures have provided useful insight into the conformational changes in this domain, they do not contain the primary functional part of the protein, namely the ion channel segments. Thus it is still unknown if these changes observed in the crystal structures and LRET investigations of the isolated domain are physiologically relevant structural changes. In order to determine the conformational changes in the receptor (histag-ΔN*-AMPA-S653C receptor), the AMPA receptors were modified as outlined in the experimental procedures section to allow the introduction of fluorophores at the sites reflecting

the cleft closure conformational change. The histag-ΔN*-AMPA-S653C receptor was characterized using radioactive ligand binding and electrophysiology to establish its functionality. Radioactive binding was performed using membrane preparations of the oocytes (Figure 3), and the K_d for AMPA was determined to be 88 ± 10 nM. This value is similar to the value of 40 ± 15 nM for the wild type receptor, showing that the AMPA binding property of the histag-ΔN*-AMPA-S653C receptor is similar to that of the wild type protein (8). To characterize the function, two electrode voltage clamp experiments were performed using oocytes expressing the modified AMPA receptor construct (Figure 3). Robust currents were obtained using 1 mM glutamate and 1 mM kainate when desensitization was blocked using 100 μM cyclothiazide. Furthermore, the dose response curve for glutamate activation of the modified protein was found to have an EC_{50} of 310 μM, similar to the EC_{50} value of 250 μM for the ΔN*-AMPA receptor (data not shown).

Having established the functionality of the modified AMPA receptors, these receptors were then used for LRET investigations. The modified AMPA receptor expressed in oocytes was tagged with the maleimide derivative of the terbium chelate, and $(Ni\text{-}NTA)_2Cy3$ was added to the membrane preparations. The lifetimes for the sensitized emission due to LRET between terbium chelate and $(Ni\text{-}NTA)_2Cy3$ were measured before and after addition of TAGZyme (Figure 4). The difference in the LRET lifetime before and after addition of the TAGZyme could be well represented by single lifetimes of 260 μs, 165 μs, and 190 μs in the apo, glutamate-bound, and kainate-bound states, respectively (Figure 4). These changes in the FRET measurements corresponded to a distance change of 4 Å between the apo and glutamate-bound states and 2 Å between apo and kainate-bound states (Table 1). The error in the absolute distances is ±2; hence the changes between apo and glutamate-bound states are significant, while the changes in the apo and kainate-bound states are not. However, as noted in the experimental procedures section, the error reported is for the absolute distance changes; the relative errors between the various ligated states for a given protein are expected to be less, since the main contributor for the error is the error in the orientation factor, which is not expected to be different between the various ligated states of the protein.

The distance change in the receptor having the transmembrane segments is in good agreement with the change observed in the investigations with the isolated ligand-binding domain, clearly indicating that the ligand binding domain in the presence of the transmembrane segments undergoes similar conformational changes as seen in the isolated ligand binding domain. It has been previously shown by crystallographic measurements that glutamate binding to the ligand binding domain of the AMPA receptor leads to a cleft closure conformational change (6,8). This cleft closure conformational change is reflected as a 6 Å distance change between the N-terminus and residue 652 in GluR2-LBD, and these distances are not significantly different from those observed in the soluble domain taking into consideration the error in the LRET measurements. Additionally, the distance changes in the LRET measurements are between a histidine tag and site 652, while the crystal structures do not have a histidine tag, thus possibly accounting for the small differences in the trends in distance change. It is also possible that in the absence of the crystallographic constraints, the changes of the ligand binding domain are smaller relative to what is seen in the crystal structures. Overall, the differences in the crystal structures and the LRET measurements are not significant, and the trends seen are the same in both.

While establishing the validity of the structural changes observed in the isolated ligand binding domain, the experiments outlined here also clearly establish the feasibility of studying conformational changes in the receptor, opening the door for future investigations on sites that are outside the ligand binding domain for which little structural information is known.

Supplementary Material

Refer to Web version on PubMed Central for supplementary material.

ACKNOWLEDGMENTS

We would like to thank Dr. Mark Mayer for assistance with the two electrode voltage clamp measurements.

This work was supported by National Science Foundation grant MCB-04444352, and National Institutes of Health Grant R01GM073102. J.G. was supported by National Institutes of Health-NRSA-GM082023-01.

Abbreviations

AMPA, α-amino-5-methyl-3-hydroxy-4-isoxazolepropionic acid; GluR2, glutamate receptor subunit 2; GluR4, glutamate receptor subunit 4; LRET, luminescence resonance energy transfer; $(Ni\text{-}NTA)_2Cy3$, bis cyanine derivative of nickel nitrilotriacetic acid..

REFERENCES

1. Mayer ML, Armstrong N. Structure and function of glutamate receptor ion channels. Annu Rev Physiol 2004;66:161–181. [PubMed: 14977400]
2. Oswald RE. Ionotropic glutamate receptor recognition and activation. Adv Protein Chem 2004;68:313–349. [PubMed: 15500865]
3. Gouaux E. Structure and function of AMPA receptors. J Physiol 2004;554:249–253. [PubMed: 14645452]
4. Mayer ML. Glutamate receptor ion channels. Curr Opin Neurobiol 2005;15:282–288. [PubMed: 15919192]
5. Mayer ML. Glutamate receptors at atomic resolution. Nature 2006;440:456–462. [PubMed: 16554805]
6. Armstrong N, Gouaux E. Mechanisms for activation and antagonism of an AMPA-sensitive glutamate receptor: crystal structures of the GluR2 ligand binding core. Neuron 2000;28:165–181. [PubMed: 11086992]
7. Jayaraman V, Keesey R, Madden DR. Ligand--protein interactions in the glutamate receptor. Biochemistry 2000;39:8693–8697. [PubMed: 10913279]
8. Armstrong N, Mayer M, Gouaux E. Tuning activation of the AMPA-sensitive GluR2 ion channel by genetic adjustment of agonist-induced conformational changes. Proc Natl Acad Sci USA 2003;100:5736–5741. [PubMed: 12730367]
9. Cheng Q, Thiran S, Yernool D, Gouaux E, Jayaraman V. A vibrational spectroscopic investigation of interactions of agonists with GluR0, a prokaryotic glutamate receptor. Biochemistry 2002;41:1602–1608. [PubMed: 11814354]
10. McFeeters RL, Oswald RE. Structural mobility of the extracellular ligand-binding core of an ionotropic glutamate receptor. Analysis of NMR relaxation dynamics. Biochemistry 2002;41:10472–10481. [PubMed: 12173934]
11. McFeeters RL, Oswald RE. Emerging structural explanations of ionotropic glutamate receptor function. Faseb J 2004;18:428–438. [PubMed: 15003989]
12. Jayaraman V. Spectroscopic and kinetic methods for ligand-protein interactions of glutamate receptor. Methods in enzymology 2004;380:170–187. [PubMed: 15051337]
13. Cheng Q, Jayaraman V. Chemistry and conformation of the ligand-binding domain of GluR2 subtype of glutamate receptors. J Biol Chem 2004;279:26346–26350. [PubMed: 15100219]
14. Cheng Q, Du M, Ramanoudjame G, Jayaraman V. Evolution of glutamate interactions during binding to a glutamate receptor. Nat Chem Biol 2005;1:329–332. [PubMed: 16408071]
15. Armstrong N, Jasti J, Beich-Frandsen M, Gouaux E. Measurement of conformational changes accompanying desensitization in an ionotropic glutamate receptor. Cell 2006;127:85–97. [PubMed: 17018279]

16. Oswald RE, Ahmed A, Fenwick MK, Loh AP. Structure of glutamate receptors. Curr Drug Targets 2007;8:573–582. [PubMed: 17504102]

17. Ahmed AH, Loh AP, Jane DE, Oswald RE. Dynamics of the S1S2 glutamate binding domain of GluR2 measured using 19F NMR spectroscopy. J Biol Chem 2007;282:12773–12784. [PubMed: 17337449]

18. Madden DR, Cheng Q, Thiran S, Rajan S, Rigo F, Keinanen K, Reinelt S, Zimmermann H, Jayaraman V. Stereochemistry of glutamate receptor agonist efficacy: engineering a dual-specificity AMPA/kainate receptor. Biochemistry 2004;43:15838–15844. [PubMed: 15595838]

19. Mankiewicz KA, Rambhadran A, Du M, Ramanoudjame G, Jayaraman V. Role of the chemical interactions of the agonist in controlling alpha-amino-3-hydroxy-5-methyl-4-isoxazolepropionic acid receptor activation. Biochemistry 2007;46:1343–1349. [PubMed: 17260963]

20. Mankiewicz KA, Jayaraman V. Glutamate receptors as seen by light: spectroscopic studies of structure-function relationships. Brazilian journal of medical and biological research 2007;40:1419–1427. [PubMed: 17934637]

21. Mankiewicz KA, Rambhadran A, Wathen L, Jayaraman V. Chemical interplay in the mechanism of partial agonist activation in alpha-amino-3-hydroxy-5-methyl-4-isoxazolepropionic acid receptors. Biochemistry 2008;47:398–404. [PubMed: 18081322]

22. Ramanoudjame G, Du M, Mankiewicz KA, Jayaraman V. Allosteric mechanism in AMPA receptors: A FRET-based investigation of conformational changes. 2006;103:10473–10478.

23. Hollmann M, Heinemann S. Cloned glutamate receptors. Annual Review of Neuroscience 1994;17:31–108.

24. Partin KM, Fleck MW, Mayer ML. AMPA receptor flip/flop mutants affecting deactivation, desensitization, and modulation by cyclothiazide, aniracetam, and thiocyanate. J Neurosci 1996;16:6634–6647. [PubMed: 8824304]

25. Sun Y, Olson R, Horning M, Armstrong N, Mayer M, Gouaux E. Mechanism of glutamate receptor desensitization. Nature 2002;417:245–253. [PubMed: 12015593]

26. Du M, Reid SA, Jayaraman V. Conformational changes in the ligand-binding domain of a functional ionotropic glutamate receptor. J Biol Chem 2005;280:8633–8636. [PubMed: 15632199]

27. Pasternack A, Coleman SK, Jouppila A, Mottershead DG, Lindfors M, Pasternack M, Keinanen K. alpha -Amino-3-hydroxy-5-methyl-4-isoxazolepropionic Acid (AMPA) Receptor Channels Lacking the N-terminal Domain. J Biol Chem 2002;277:49662–49667. [PubMed: 12393905]

28. Mannuzzu LM, Moronne MM, Isacoff EY. Direct physical measure of conformational rearrangement underlying potassium channel gating. Science 1996;271:213–216. [PubMed: 8539623]

29. Posson DJ, Ge P, Miller C, Bezanilla F, Selvin PR. Small vertical movement of a K+ channel voltage sensor measured with luminescence energy transfer. Nature 2005;436:848–851. [PubMed: 16094368]

30. Kapanidis AN, Ebright YW, Ebright RH. Site-specific incorporation of fluorescent probes into protein: hexahistidine-tag-mediated fluorescent labeling with (Ni(2+):nitrilotriacetic Acid (n)-fluorochrome conjugates. J Am Chem Soc 2001;123:12123–12125. [PubMed: 11724636]

31. Haas E, Katchalski-Katzir E, Steinberg IZ. Effect of the orientation of donor and acceptor on the probability of energy transfer involving electronic transitions of mixed polarization. Biochemistry 1978;17:5064–5070. [PubMed: 718874]

32. Selvin PR. Principles and biophysical applications of lanthanide-based probes. Annu Rev Biophys Biomol Struct 2002;31:275–302. [PubMed: 11988471]

33. Armstrong N, Sun Y, Chen GQ, Gouaux E. Structure of a glutamate-receptor ligand-binding core in complex with kainate. Nature 1998;395:913–917. [PubMed: 9804426]

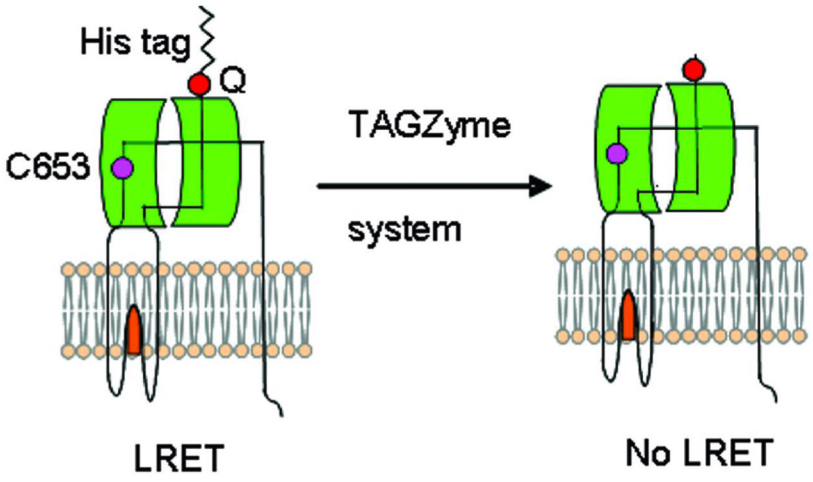

Figure 1.

A schematic representation of the experiments performed with the AMPA receptors expressed in oocytes. The modified GluR4 homomeric AMPA receptor had a histidine tag followed by a glutamine residue introduced at the N-terminus (histag-ΔN*-AMPA-S653C receptor). LRET was measured between the site C653 and the histidine tag before and after TAGZyme digestion, with glutamine acting as the stop site for the enzyme.

Figure 2.

LRET lifetimes as measured by the sensitized emission of the acceptor at 575 nm before and after thrombin digestion in the apo state for (I) the supernatant from *E. Coli* cell lysate and (II) purified GluR2-LBD. The difference between the lifetimes obtained before and after digestion with thrombin in the apo and glutamate-bound states for (III) the supernatant from *E. C*oli cell lysate and (IV) purified GluR2-LBD.

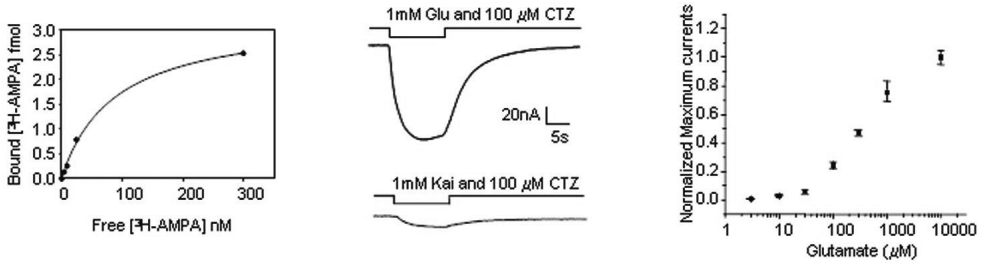

Figure 3.

Functional characterization of the histag-ΔN*-AMPA-S653C receptors. (A) Radioactive ligand binding showing [^{3}H]-AMPA binding to membrane preparations of oocytes expressing histag-ΔN*-AMPA-S653C. (B) Two electrode voltage clamp experiments performed with oocytes expressing histag-ΔN*-AMPA-S653C receptors. Representative currents recorded with 1 mM glutamate in the presence of cyclothiazide and 1 mM kainate in the presence of cyclothiazide. (C) Dose response curve showing the dependence of the maximum current as a function of glutamate concentration for the histag-ΔN*-AMPA-S653C receptors. All currents were recorded in the presence of cyclothiazide and normalized to currents mediated by 10 mM glutamate.

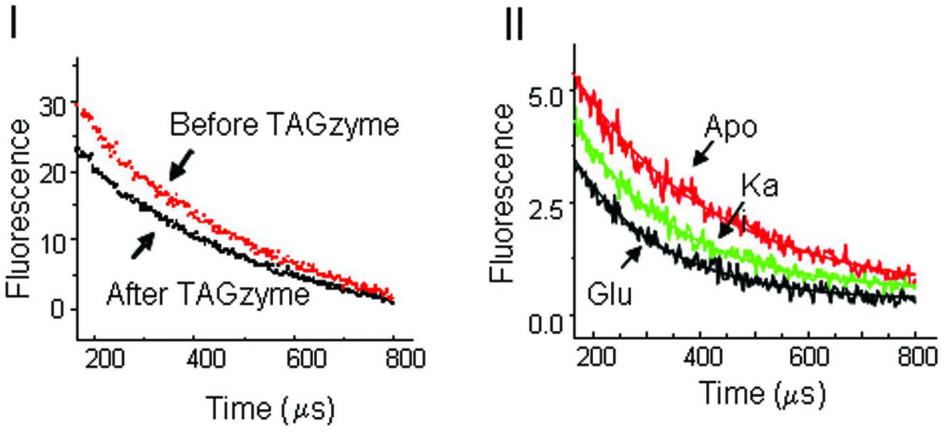

Figure 4.

(I) LRET lifetimes as measured by the sensitized emission of the acceptor at 575 nm before and after TAGZyme digestion in the apo state for the modified AMPA receptor. (II) The difference between the lifetimes obtained before and after digestion with TAGZyme in the apo, glutamate-bound, and kainate-bound states.

Table 1

The fluorescence lifetimes and distances for GluR2-LBD and histag-ΔN*-AMPA-S653C receptors.

Protein	Ligand	Donor lifetime (μs)	Sensitized emission lifetime (μs)	Distance (Å)
GluR2-LBD supernatant	Apo	1590±45	240±20	51±2
GluR2-LBD supernatant	Glutamate	1575±60	145±10	46±2
GluR2-LBD purified protein	Apo	1490±40	210±10	51±2
GluR2-LBD purified protein	Glutamate	1455±65	130±10	46±2
histag-ΔN*-AMPA-S653C receptor	Apo	1575±60	260±25	51±2
histag-ΔN*-AMPA-S653C receptor	Glutamate	1580±45	165±15	47±2
histag-ΔN*-AMPA-S653C receptor	Kainate	1585±45	190±10	49±2